Supporting Information

A Microfluidic Cathodic Photoelectrochemical Biosensor Chip for Targeted Detection of Cytokeratin 19 Fragments 21-1

Jinhui Feng,[a] Tingting Wu,[a] Qian Cheng,[a] Hongmin Ma,[a] Xiang Ren,*[a] Xueying Wang,[a] Jin Yong Lee,[b] Qin Wei,*[a] Huangxian Ju*[a]

a Collaborative Innovation Center for Green Chemical Manufacturing and Accurate Detection, Key Laboratory of Interfacial Reaction & Sensing Analysis in Universities of Shandong, School of Chemistry and Chemical Engineering, University of Jinan, Jinan 250022, PR China

b Department of Chemistry, Sungkyunkwan University, Suwon, 16419, Republic of Korea.

Corresponding Authors

E-mail: chem_renx@163.com (Xiang Ren)

sdjndxwq@163.com (Qin Wei)

hxju@nju.edu.cn (Huangxian Ju)

Table of Contents:

Materials. The antigen of CYFRA 21-1, capture-antibody (Ab_1), detection antibody (Ab_2), and antigens of SCCA, PSA, PCT, BNP were all purchased from Shanghai Linc-Bio Science Co. LTD (Shanghai, China). Bovine serum albumin (BSA) (96– 99%) were purchased from Sigma-Aldrich Co. (St. Louis, MO, USA). Bismuth nitrate pentahydrate ($Bi(NO_3)_3 \cdot 5H_2O$), silver nitrate ($AgNO_3$), gallium oxide (Ga_2O_3, 99.999%) and superoxide dismutase (SODs) were purchased from Macklin Reagent Co. Ltd. (Shanghai, China). Potassium iodide (KI), potassium permanganate ($KMnO_4$) and 3-aminopropyltriethoxysilane (APTES) were obtained from Shanghai Reagent Company (Beijing, China). All of the other chemicals were of analytical reagent grade and were used without further purification. Indium tin oxide (ITO) (resistivity 10 Ω/sq) glass was obtained from Zhuhai Kaivo Electronic Components Co. Ltd., China. 5 mM $K_3Fe(CN)_6/K_4Fe(CN)_6$ and 0.1 M KNO_3 solution were used as electrolyte for electrochemical impedance spectroscopy (EIS). Tris(hydroxymethyl)aminomethane (Tris-HCl) (0.1 M) with the pH value of 6.8 was always employed as electrolyte buffer.

Apparatus. Scanning electron microscope (SEM) images was applied by a field emission SEM (Zeiss, Germany). The JEOL JEM-2100F transmission electron microscope (TEM) (Japan) was used for the characterization of TEM and HRTEM images. X-ray photoelectron spectroscopy (XPS) analysis was performed on ESCALAB 250 X-ray

photoelectron spectrometer with an Al Kα radiation source (1486.6 eV). X-ray diffraction (XRD) patterns were performed with D8 advance X-ray diffractometer (Bruker AXS, Germany). UV-vis diffuse reflectance spectrum measurements were performed with a Shimadzu UV-3101PC spectrometer (Japan). Electrochemical impedance spectra (EIS) were performed using an electrochemical workstation (Zahner Zennium PP211, Germany). Soft lithography method was performed using a Mask Aligner (Institute of Optics and Electronics, Chinese Academy of Sciences URE 2000-30, China).

Preparation of microfluidic microelectrode. Firstly, ITO was cut into 6 cm ×5 cm slices as substrate for the fabrication wet etching on ITO slices according to published work. Thereafter, ITO was thoroughly cleaned by detergent, ultrapure water, acetone and absolute ethyl alcohol, respectively. After drying at 70 ˚C for 4 h, oil ink was printed on the conductive surface of ITO substrate through the silk-screen mode, then dried at 80 ˚C overnight. To obtain the developed working electrode, oil ink-protected ITO substrate was etched through wet chemical etching method with etching solution ($FeCl_3$: HNO_3: HCl=0.5 M: 1 M: 1 M) at 37 ˚C for 20 min to remove the conductive layer without oil ink protected parts, followed by washing with ultrapure water. These etched ITO substrates were immersed in acetone to remove the oil ink. To further clean these ITO substrates, first they were immersed in 200 mL ethyl alcohol ultrasonic for 2 h, then were immersed in 200 mL isopropanol containing 2 M KOH solution under boiling 15 min, then thoroughly washed with ultrapure water.

Finally, the polydimethylsiloxane (PDMS) microchannels of desired dimensions (6 cm × 2000 μm × 300 μm) and microelectrodes composed of dimensions (300 × 3000 μm^2) were fabricated using soft lithographic technique. The inlet and outlet were fabricated by punching holes at the ends of the microchannel. Then, the prepared p-n AgI/$Bi_2Ga_4O_9$ WE, containing the counter electrode (CE) and reference electrode (RE) and

PDMS microchannels were treatment with oxygen plasma for 50 s, and then stick together.

Preparation of $hMnO_2$. In details, 0.3 g of $KMnO_4$ was dissolved in 150 mL of ultrapure water, and then the mixture was stirred for about 0.5 h. After that, 3 mL of oleic acid (OA) was added into the resulting mixture solution for reacting 24 h. Finally, a crude brown product was collected by centrifugation, washed several times with ultrapure water and alcohol. Specially, $hMnO_2$ nanostructures were produced at the oil/water interface via the redox reaction between $KMnO_4$ and OA.

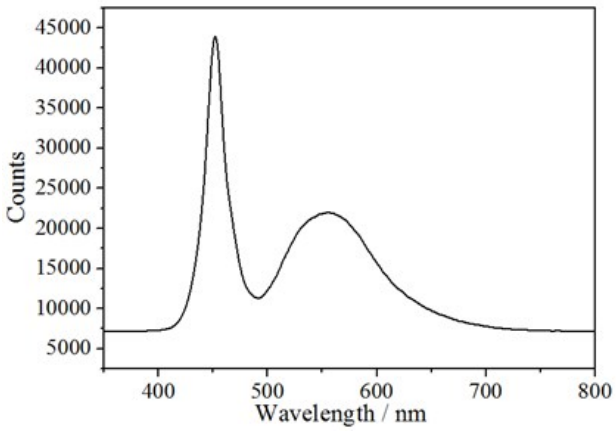

Fig S1. Wavelength range of the stimulation resource.

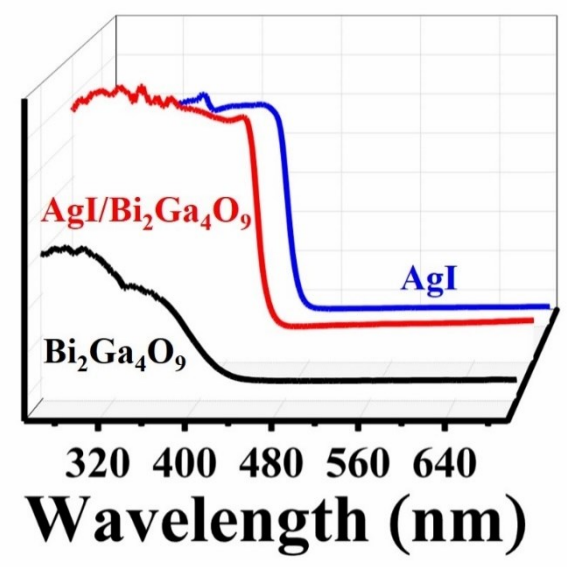

Fig S2. UV–vis diffuse reflectance spectra of $Bi_2Ga_4O_9$, AgI, and AgI/$Bi_2Ga_4O_9$.

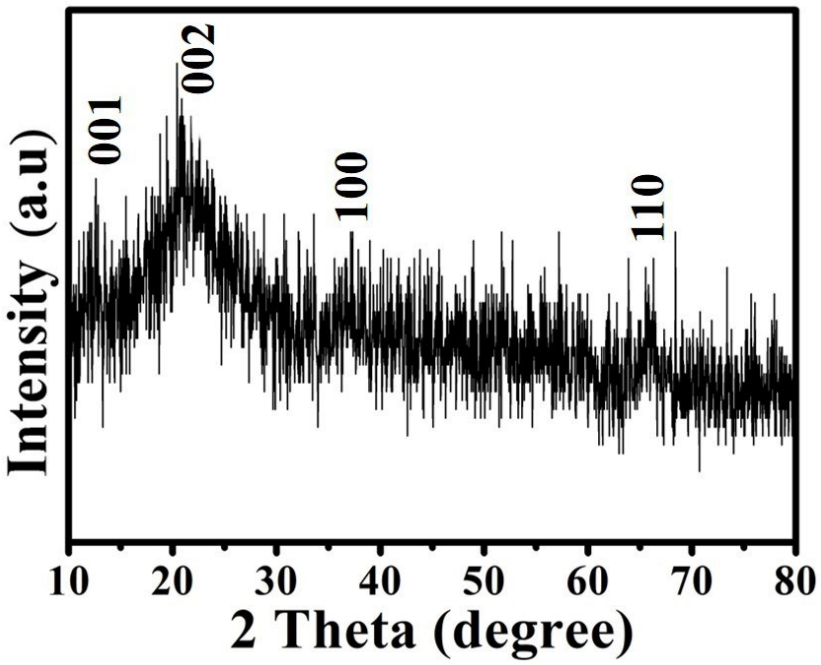

Fig S3. XRD patterns of $hMnO_2$.

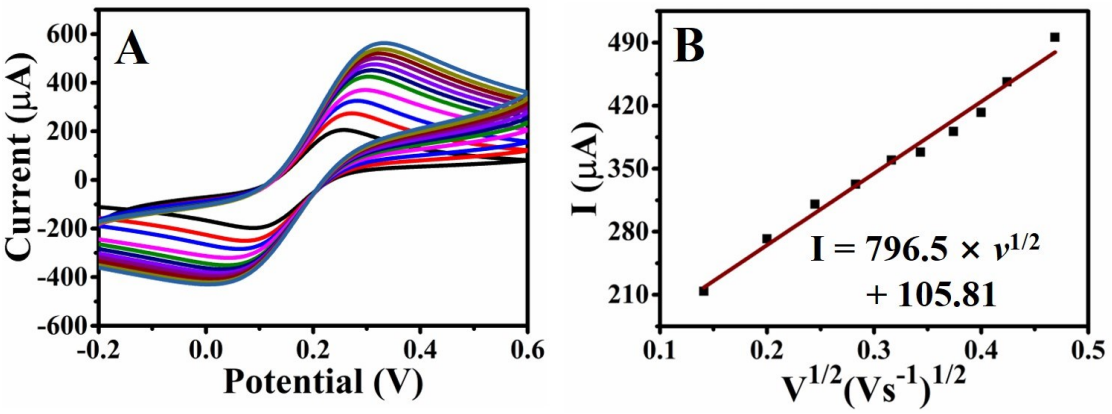

Fig S4. CV detections of (A) bare WE in $[Fe(CN)_6]^{4-/3-}$ solution; Linear relation between the peak reduction current I and $v^{1/2}$ of (B).

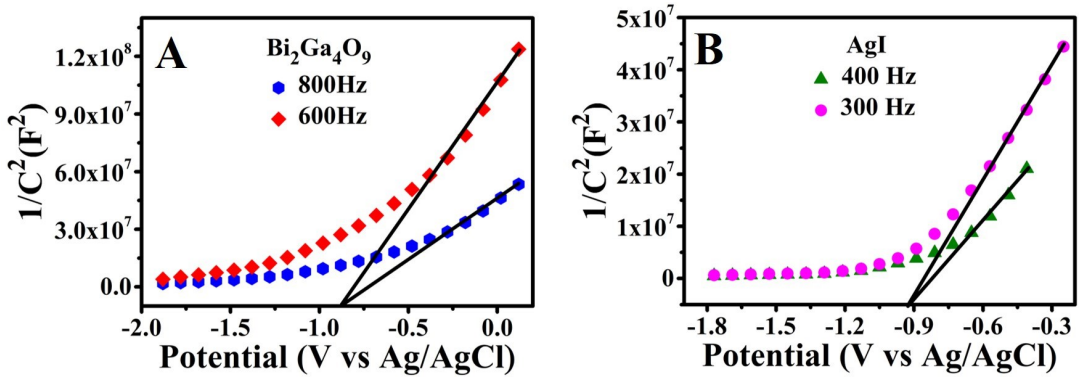

Fig S5. Mott-Schottky plots of $Bi_2Ga_4O_9$ (A) and AgI (B) in a 0.2 mol/L Na_2SO_4 aqueous solution.

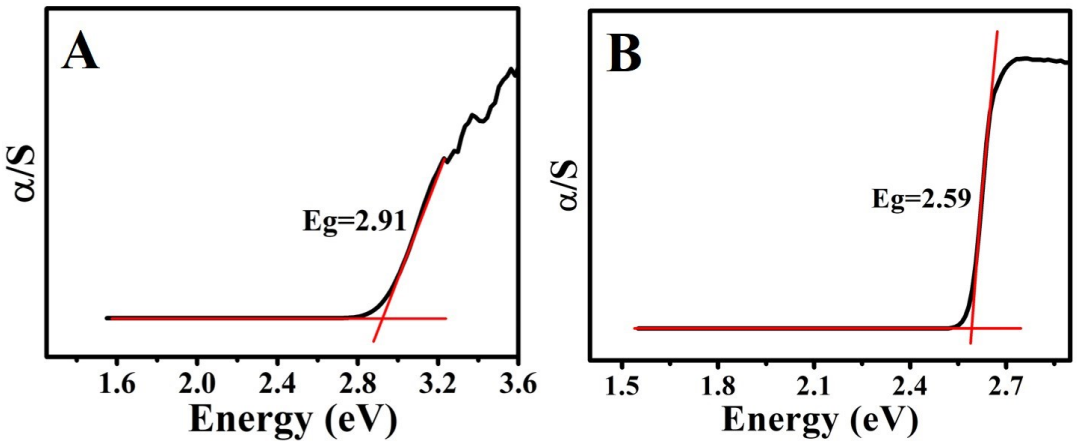

Fig S6. UV-vis diffuse reflectance spectra of $Bi_2Ga_4O_9$ (A) and AgI (B).

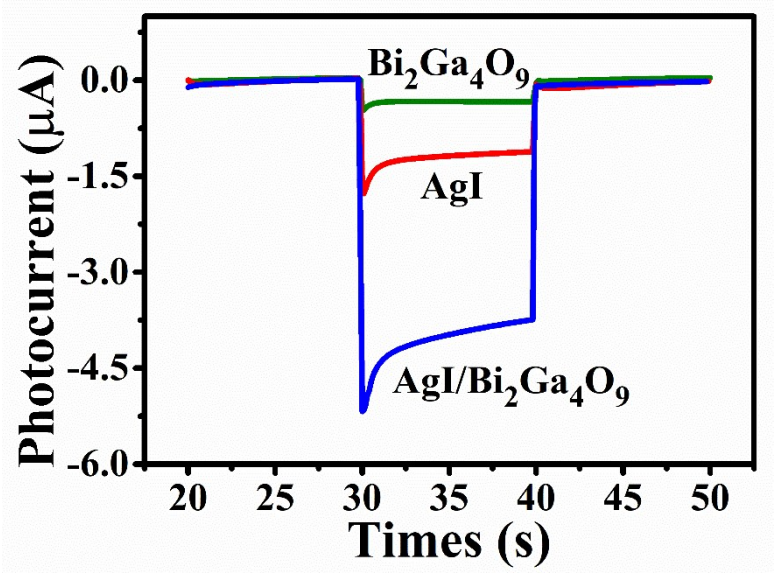

Fig S7. The cathodic photocurrent of AgI, $Bi_2Ga_4O_9$, and p-n AgI/$Bi_2Ga_4O_9$.

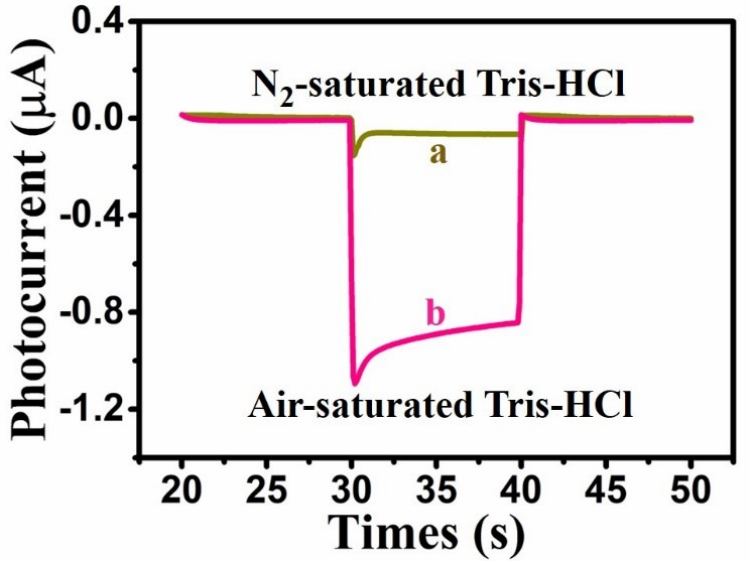

Fig S8. PEC signals of fabricated biosensor in N_2-satuated Tris-HCl solution and Air-saturated Tris-HCl solution.

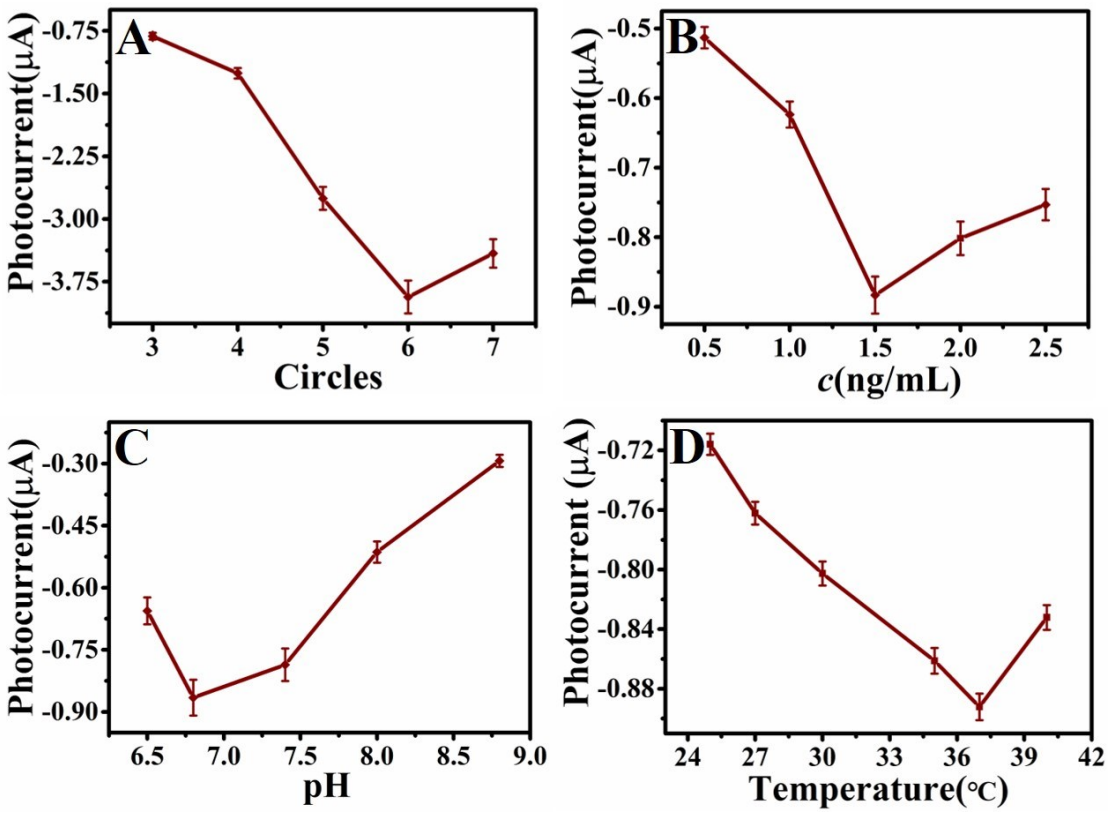

Fig S9. Optimization of experimental conditions: (A) electrodeposition circles for AgI; (B) concentration of SODs@hMnO_2-Ab_2; (C) pH value; (D) temperature of AA.

Optimization of Experimental Conditions. For the best sensing performances for cathodic PEC microfluidic biosensor, four major experiment conditions were optimized one by one, including electrodeposition circles for AgI, concentration of SODs@hMnO_2-Ab_2, pH value and concentration for AA in Fig. S9.

The cathodic photocurrent response of this developed biosensor was influenced by the electrodeposition circles for AgI. As shown in Fig. S9A, it was found that the absolute photocurrent value was maximum when the electrodeposition circles at six. Therefore, the electrodeposition circles of six was adopted as the optimal circles for AgI electrodeposition in this work.

The cathodic photocurrent response increased with concentration of SODs@hMnO_2-Ab_2 from 0.5 to 2.5 mg/mL, followed by a decrease with concentration from 1.5 to 2.5 mg/mL in Fig. S9B. It is inferred that the increased of SODs@hMnO_2 film thickness might increase interface electron resistance. Thus, the optimal concentration of SODs@hMnO_2 was 1.5 mg/mL in this work.

The pH of base solution has a great influence on the immunosensor because of alkaline or acid solutions may break the antigen-antibody. To optimize the pH, a series of 0.1 M Tris-HCl solution with the pH from 6.5 to 9.0 was investigated. As shown in Fig. S9C, the cathodic photocurrent response increased from pH 6.5-6.8 and then decreased. Therefore,

pH=6.8 Tris-HCl solution was appropriate for the test.

The temperature also has an influence on cathodic photocurrent response. As shown in Fig. S9D, the cathodic photocurrent signal increased as the temperature was increased from 25 to 37 ˚C, followed by a decrease when the temperature was increased from 37 to 40 ˚C. It is expected that the activity of antigens and antibodies could be affected when the temperature is higher than 37 ˚C. Therefore, the optimal temperature of fabricated biosensor was at 37 ˚C.

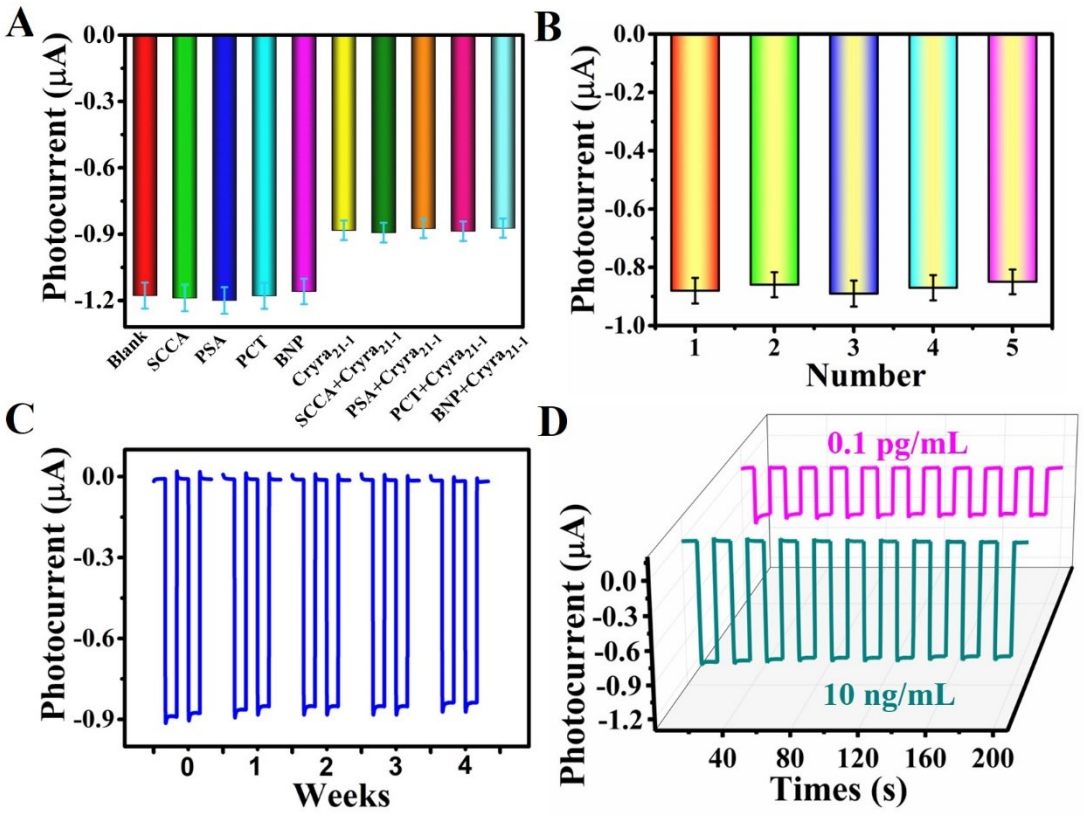

Fig S10. (A) The cathodic PEC current of CYFRA 21-1 (1 ng/mL) alone and compound of interfering substances (100 ng/mL); (B) The reproducibility of five cathodic PEC biosensor; (C) The storage stability of the CYFRA 21-1 biosensor. (D) The stability of the fabricated cathodic PEC biosensor.

Specificity, Reproducibility, and Stability of Cathodic PEC Microfluidic Biosensor. Specificity is an important criterion for fabricated cathodic PEC biosensor, due to the nonspecific binding could influence the accuracy of the detection results. To validate that the photocurrent response originated from specific binding of immunoreactions, some typical interfering substances including SCCA, PSA, PCT, and BNP were measured under the optimal conditions for the interference test. The cathodic PEC response of the biosensor in Fig. S10A showed the 1 ng/mL CYFRA 21-1 detection was not affected by the mixture of 100 ng/mL with SCCA, PSA, PCT, and BNP. Compared to the cathodic photocurrent response demonstrated that the proposed cathodic PEC biosensor has a satisfactory specificity without obvious interference from nonspecific binding.

Reproducibility is a significant indicator to evaluate the precision of the designed cathodic PEC biosensor. To evaluate the reproducibility, five parallel fabricated biosensors were prepared to detect the cathodic PEC biosensor (1 ng/mL of CYFRA 21-1) by relative standard deviation (RSD). Calculated from the detection results with five parallel tests, the within batch RSD were 1.14% toward 1 ng/mL (the samples 1-5) in Fig. S10B. The result implied that the designed cathodic PEC biosensor has a remarkable reproducibility.

The storage stability of prepared biosensor was shown in Fig. S10C,

the cathodic photocurrent intensity was maintained 97.7%, 95.4%, and 94.3% of its initial response after storage for 2 weeks, 3 weeks and 4 weeks respectively, implying that the designed biosensor has acceptable storage stability. Fig. S10D showed the stability of the cathodic photocurrent response of the fabricated biosensor. The cathodic photocurrent response of the biosensor was repeated 10 times on/off irradiation cycles with incubating 1 ng/mL CYFRA 21-1. There was no noticeable variation occurred, implying the cathodic PEC biosensor possesses stable photocurrent response for CYFRA 21-1 detection.

Table S1. Comparison of different methods for the detection of CYFRA 21-1

Method	Linear range	Detection limit	Reference
Electrochemical Immunosensor	0.25-800 ng/mL	100 pg/mL	[1]
Electrochemical Immunosensor	2-22 ng/mL	122 pg/mL	[2]
ECL Immunosensor	0.0005-50 ng/mL	0.14 pg/mL	[3]
ECL Immunosensor	0.0075-50 ng/mL	1.89 pg/mL	[4]
PEC Immunosensor	0.01-100 ng/mL	2.5 pg/mL	[5]
Fluorescence Immunosensor	1.3-480 ng/mL	160 pg/mL	[6]
Cathodic PEC biosensor	1×10^{-4}-100 ng ml^{-1}	0.026 pg/ml	This method

References

1. A, Y. Z.; A, J. B.; A, Y. Z.; B, D. H.; A, M. C.; A, M. Y.; C, H. F.; A, C. H., *Talanta* **2018,** *178*, 122.

2. Kumar, S.; Sharma, J. G.; Maji, S.; Malhotra, B. D., *Biosens Bioelectron* **2016,** *78*, 497-504.

3. Du, Y.; Xue, J.; Sun, X.; Wu, D.; Liu, X.; Ju, H.; Yang, L.; Wei, Q., *Anal Chem* **2020,** *92* (12), 8472-8479.

4. Li, X.; Du, Y.; Wang, H.; Ma, H.; Wu, D.; Ren, X.; Wei, Q.; Xu, J. J., *Anal Chem* **2020**.

5. Yu, Y.; Huang, Z.; Zhou, Y.; Zhang, L.; Liu, A.; Chen, W.; Lin, J.; Peng, H., *Biosens Bioelectron* **2019,** *126*, 1-6.

6. Chen, Z.; Liang, R.; Guo, X.; Liang, J.; Deng, Q.; Li, M.; An, T.; Liu, T.; Wu, Y., *Biosens Bioelectron* **2017,** *91*, 60-65.